



Energetic electron distributions fitted with a relativistic kappa-type function at geosynchronous orbit

Fuliang Xiao,¹ Chenglong Shen,² Yuming Wang,² Huinan Zheng,² and Shui Wang²

Received 23 October 2007; revised 29 December 2007; accepted 5 February 2008; published 3 May 2008.

[1] In this study, we utilize a recently introduced relativistic kappa-type (KT) distribution function to model the omnidirectional differential flux of energetic electrons observed by the SOPA instrument on board the 1989–046 and LANL-01A satellites at geosynchronous orbit. We derive a useful correlation between the differential flux and the distribution of particles which can directly offer those best fitting parameters (e.g., the number density N , the thermal characteristic speed θ and the spectral index κ) strongly associated with evaluation of the electromagnetic wave instability. We adopt the assumption of a nearly isotropic pitch angle distribution (PAD) and the typical LMFIT function in the program IDL to perform a non-linear least squared fitting, and find that the new KT distribution fits well with the observed data during different universal times both in the lower and higher energies. We also carry out the direct comparisons with the generalized Lorentzian (kappa) distribution and find that kappa distribution fits well with observational data at the relatively lower energies but display deviations at higher energies, typically above hundreds of keV. Furthermore, the fitting spectral index κ basically takes 4, 5 or 6 while the fitting parameters N and θ are quite different due to different differential fluxes of electrons at different universal times. These results, which are applied to the case of a nearly isotropic PAD, demonstrate that the particle flux satisfies the power law not only at the lower energies but also at the relativistic energies, and the new KT distribution may present valuable insights into the dynamical features in those space plasmas (e.g., the Earth's outer radiation belts and the inner Jovian magnetosphere) where highly energetic particles exist.

Citation: Xiao, F., C. Shen, Y. Wang, H. Zheng, and S. Wang (2008), Energetic electron distributions fitted with a relativistic kappa-type function at geosynchronous orbit, *J. Geophys. Res.*, 113, A05203, doi:10.1029/2007JA012903.

1. Introduction

[2] Through the cyclotron wave-particle interaction, energetic electrons (with energies \sim several hundreds of keV or above) have been found to play a fundamental role in the dynamics of the space plasma, see the reviews by *Gendrin* [2001], *Horne* [2002], and *Thorne et al.* [2005a]. An important acceleration mechanism for outer radiation belt energetic electrons is recognized to be the inward radial diffusion through drift resonance with ULF waves [*Li et al.*, 1999, 2001; *Li and Temerin*, 2001; *Li*, 2004; *Barker et al.*, 2005; *Sarris et al.*, 2006]. However, there has been increasing evidence that the cyclotron wave-particle interaction is also primarily responsible for the stochastic acceleration and pitch angle scattering of energetic electrons during the

geomagnetic storms [*Summers et al.*, 1998, 2001, 2004, 2007a, 2007b; *Roth et al.*, 1999; *Summers and Ma*, 2000; *Meredith et al.*, 2002, 2003a; *Horne et al.*, 2003a, 2005a, 2005b; *Summers and Thorne*, 2003; *Li et al.*, 2005a; *Xiao et al.*, 2006a, 2007a]. Since the energetic electron flux in the Earth's outer radiation belt is highly variable, particularly during geomagnetic storms or other geomagnetic disturbances [*Li et al.*, 1997, 2005b; *Reeves et al.*, 1998, 2003; *Zong et al.*, 2007], those energetic ("killer") electrons have been found to yield the failure and malfunctions of geostationary spacecraft [e.g., *Baker*, 2002], or precipitate into the atmosphere and change atmospheric chemistry, leading to ozone destruction [*Thorne*, 1977; *Callis et al.*, 1998]. Therefore specifying and even forecasting the fluxes of those energetic electrons during and following geomagnetic storms constitute important facets of space weather science. One important way is to establish their relationships to the lower-energy electrons which can already be well fitted.

[3] Electromagnetic wave instability (e.g., whistler mode and EMIC waves), which primarily controls the timescales for the stochastic acceleration and pitch angle scattering processes [*Meredith et al.*, 2003b; *Horne et al.*, 2003b; *Thorne et al.*, 2005b], is found to be associated with the behavior of particle distributions or fluxes [*Gary and Wang*,

¹School of Physics and Electronic Sciences, Changsha University of Science and Technology, Changsha, China.

²Chinese Academy of Sciences Key Laboratory for Basic Plasma Physics, School of Earth and Space Sciences, University of Science and Technology of China, Hefei, China.

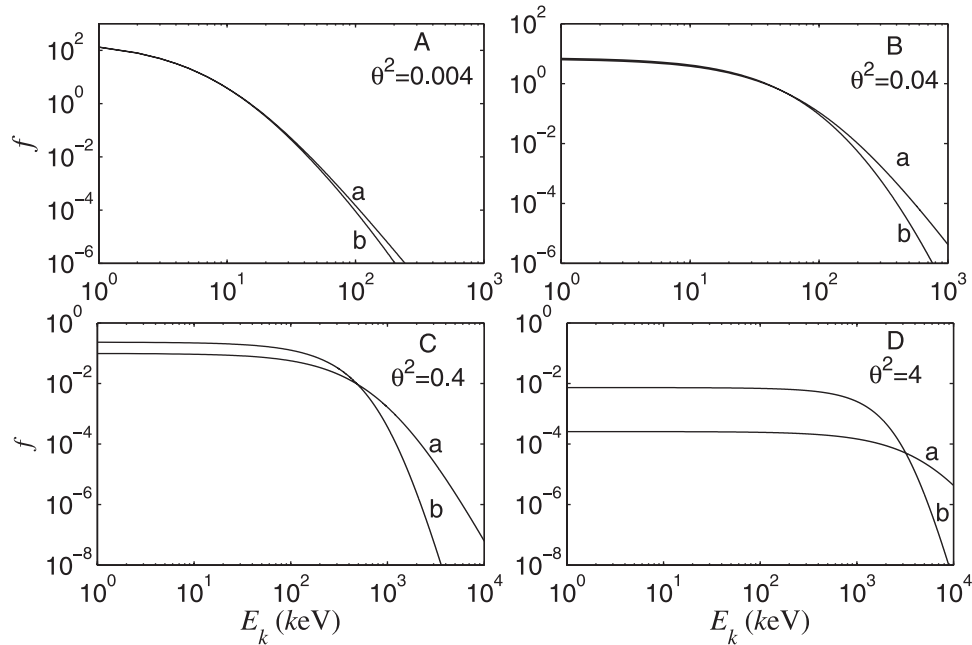


Figure 1. Distribution function curves for the KT (a) and the kappa (b) for the indicated values of θ^2 and $\kappa = 5$. Since θ^2 is scaled by $m_e c^2 \approx 500$ keV, θ^2 approximately corresponds to 2 keV, 20 keV, 200 keV, 2 MeV respectively.

1996; Gary *et al.*, 2000, 2005; Xiao *et al.*, 2006b, 2007b]. The typically hot, tenuous and collisionless space plasmas generally has a power law tail in energy and basically can be well fitted with a generalized Lorentzian (kappa) distribution [Vasyliunas, 1968; Christon *et al.*, 1988; Viñas *et al.*, 2005]. So far, the typical kappa distribution has been extensively used in numerous previous papers [e.g., Dasso *et al.*, 2003; Saito *et al.*, 2000; Xue *et al.*, 1993; Maksimovic *et al.*, 1997a, 1997b] to model the high energetic particles behavior. Various observational data have demonstrated that the electrons from 100 keV to 1.5 MeV can be well characterized by a power law spectrum at geostationary orbit for the November 1993 geomagnetic storm [Freeman *et al.*, 1998], the energy spectrum of electron measurements from the LANL satellites and from GOES 10 is best described by a power law index [Burin des Roziers and Li, 2006], and the energy spectra of ions accelerated in impulsive and gradual solar events can be fitted to a power law [Reames *et al.*, 1997]. The possible physical mechanisms associated with the power law particle distributions is considered to be stochastic acceleration by plasma wave turbulence and collisionless shocks [Ma and Summers, 1998]. However, the well-known kappa distribution satisfies the form: $\propto [1/v^2]^{(\kappa+1)}$ instead of $\propto [1/p]^{\kappa+1}$ at the relativistic energy (here v and p denote velocity and momentum of particles, respectively). This appears to be inconsistent with the power law since the relativistic energy is proportional to p instead of v^2 . Recently, Xiao [2006] developed a fully relativistic kappa-type (KT) distribution to model the highly energetic particles in a more physically realistic way in plasmas where magnetic mirror geometries occur. The new KT distribution is found to combine those features of the

well-known kappa type and loss cone type, and follow the power law at both the lower energies and the relativistic energies. Since the geostationary satellites provide a very efficient way to investigate variations in the energetic electron flux associated with substorms and other geomagnetic disturbances, in this study, we therefore revisit those observational data at geostationary orbit during different universal times and adopt the new KT distribution to model energetic electrons spectra.

2. The Fitting Method and Distribution Functions

[4] As indicated above, the present work is dedicated to the modeling of the observed energetic electron flux by the KT distribution function. In the following, we need to derive the correlation between the distribution function and the differential flux of particles in the relativistic case. The typical relation between the differential flux $j(E)$ and the distribution function $f(p)$ can be written [Schulz and Lanzerotti, 1974]:

$$j(E) = p^2 f(p) \quad (1)$$

where E is the kinetic energy of particles, and p is the momentum of particles with components p_{\parallel} and p_{\perp} , respectively, parallel and perpendicular to the ambient magnetic field. In the relativistic limit, we can write

$$p^2 = \frac{m_0 E (E + 2E_0)}{E_0} \quad (2)$$

where $E_0 (= m_0 c^2)$ is the rest mass energy of particles with $c (= 3 \times 10^{10} \text{ cm} \cdot \text{s}^{-1})$ being the speed of light.

[5] For the simplicity, we adopt the following normalization: $p_s = p/m_0 c$ and $E_s = E/E_0$. Since the total number density N is the same, we can obtain

$$N = \int f(p) d^3 p = \int f(p_s) d^3 p_s, \quad f(p) = f(p_s)/m_0^3 c^3 \quad (3)$$

here $d^3 p = 2\pi p_\perp dp_\perp dp_\parallel$ is the volume element in momentum space. Therefore we further arrive at the following relation:

$$j = \frac{cE_s(E_s + 2)}{E_0} f(p_s) \quad (4)$$

[6] Equation (4), which associates the differential flux with the distribution function in the scaled variables, constitutes the basic method for modeling the observed data. Furthermore, as will be seen below, one advantage of equation (4) is that it can directly provide those important fitting parameters associated with the evaluation of wave instability, e.g., the thermal characteristic parameter, the number density and the spectra index.

[7] The general relativistic kappa-type distribution in the scaled variables is introduced by *Xiao* [2006]:

$$f^{\kappa T}(p_s, \alpha) = \frac{N}{2\pi^{3/2}} \frac{\Gamma((q+3)/2) 1}{\Gamma((q+2)/2) I} \frac{1}{I} \cdot \left[1 + \frac{\sqrt{1+p_s^2} - 1}{\kappa\theta^2} \right]^{-(\kappa+1)} \sin^q \alpha \quad (5)$$

where I is the normalized constant given by:

$$I = \frac{8B(3/2, \kappa - 2)}{2\kappa - 1} \{ 3F(\kappa + 1, 5/2; \kappa + 1/2; 1 - 2/\kappa\theta^2) + (\kappa - 2)F(\kappa + 1, 3/2; \kappa + 1/2; 1 - 2/\kappa\theta^2) \} \quad (6)$$

where Γ , B and F represent the gamma function, the beta function and the hypergeometric function respectively, α is the particle pitch angle, q represents the pitch angle anisotropy, θ^2 is the thermal characteristic parameter scaled by $m_0 c^2$, and N is the number density of particles. The term $(\sqrt{1+p_s^2} - 1)$ appearing in equation (5) is actually the scaled kinetic energy E_s .

[8] As noted by *Xiao* [2006], the thermal anisotropy $A^{\kappa T}$ of energetic particles for the KT distribution can be defined as

$$A^{\kappa T} = \frac{\int p_{s\perp}^2 f d^3 p_s}{2 \int p_{s\parallel}^2 f d^3 p_s} - 1 = \frac{q}{2} \quad (7)$$

[9] This indicates that the KT distribution possesses the same anisotropy as a typical loss cone distribution (i.e., $\propto \sin^q \alpha$) does.

[10] Similar to the regular non-relativistic kappa distribution function adopted by previous authors [*Xue et al.*, 1993; *Saito et al.*, 2000; *Dasso et al.*, 2003], we shall use the

following kappa distribution in the scaled momentum space [*Xiao et al.*, 1998]:

$$f^\kappa(p_{s\parallel}, p_{s\perp}) = \frac{\Gamma(\kappa + l + 1)}{\pi^{3/2} \theta_\perp^2 \theta_\parallel^{\kappa(l+3/2)} \Gamma(l+1) \Gamma(\kappa - 1/2)} \left(\frac{p_{s\perp}}{\theta_\perp} \right)^{2l} \cdot \left[1 + \frac{p_{s\parallel}^2}{\kappa\theta_\parallel^2} + \frac{p_{s\perp}^2}{\kappa\theta_\perp^2} \right]^{-(\kappa+l+1)} \quad (8)$$

here l , analogous to the index “ q ” in a typical loss cone distribution (i.e., $\propto \sin^q \alpha$), represents the pitch angle anisotropy associated with a measure of the angular size of the loss cone region; θ_\parallel and θ_\perp^2 are the thermal characteristic parameters (scaled by $m_0 c^2$) associated with the temperature anisotropy. The regular kappa distribution function (8) with typical value of κ in the range between 2 and 6 is found to offer a good representation for the high energy tail population of the space plasmas.

[11] The thermal anisotropy A^κ for the kappa distribution can be written:

$$A^\kappa = \frac{(l+1)\theta_\perp^2}{\theta_\parallel^2} - 1 \quad (9)$$

[12] Equation (9) implies that the overall anisotropy for the kappa distribution combines both the loss cone and the temperature anisotropy.

[13] Following previous work [*Xiao*, 2006], we summarize some basic features of KT distribution $f^{\kappa T}(p, \alpha)$ as follows (1). If $\theta^2 \ll 1$, leading to $\sqrt{1+p^2} - 1 \approx p^2/2$, $f^{\kappa T}(p, \alpha) \propto [1 + p^2/2\kappa\theta^2]^{-(\kappa+1)}$ (or $[1 + v^2/2\kappa\theta^2]^{-(\kappa+1)}$), i.e., the KT distribution reduces to the non-relativistic kappa distribution. (2). If $\theta^2 \gg 1$, then $\sqrt{1+p^2} - 1 \approx p$, i.e., $f^{\kappa T}(p, \alpha) \propto [1 + p/\kappa\theta^2]^{-(\kappa+1)}$, indicating that the KT distribution decays with a power law at relativistic energy. (3). If $\kappa \rightarrow \infty$, then $f^{\kappa T}(p, \alpha) \propto \exp[-\sqrt{1+p^2}/\theta^2]$, implying that $f^{\kappa T}(p, \alpha)$ incorporates the features of the well-known standard relativistic Maxwellian distribution function. As a result, the energy part returns to the usual non-relativistic Maxwellian if $\theta^2 \ll 1$, and spreads at relativistic energy ($\sim \exp[-p/\theta^2]$) if $\theta^2 \gg 1$. This is consistent with the previous results [*Gladd*, 1983; *Schlickeiser et al.*, 1997].

[14] Based on those features above, *Xiao et al.* [2006c] evaluated the whistler mode instability in detail by using the KT distribution and typical kappa distribution and found that the KT and the kappa distributions have different effects on the wave growth even for the same overall anisotropy and thermal characteristic parameters. Specifically, the wave growth by the KT distribution is generally higher than that by the kappa distribution in the lower wave frequency, but lower in the higher wave frequency.

3. Results and Discussion

[15] The 1986–046 and LANL-01A satellites locate in the geosynchronous orbit which have a nominal altitude of 6.6 R_E (42,000 km). The Synchronous Orbit Particle Analyzer (SOPA) detector on board these satellites measures electrons from 50 keV to approximately 26 MeV. The

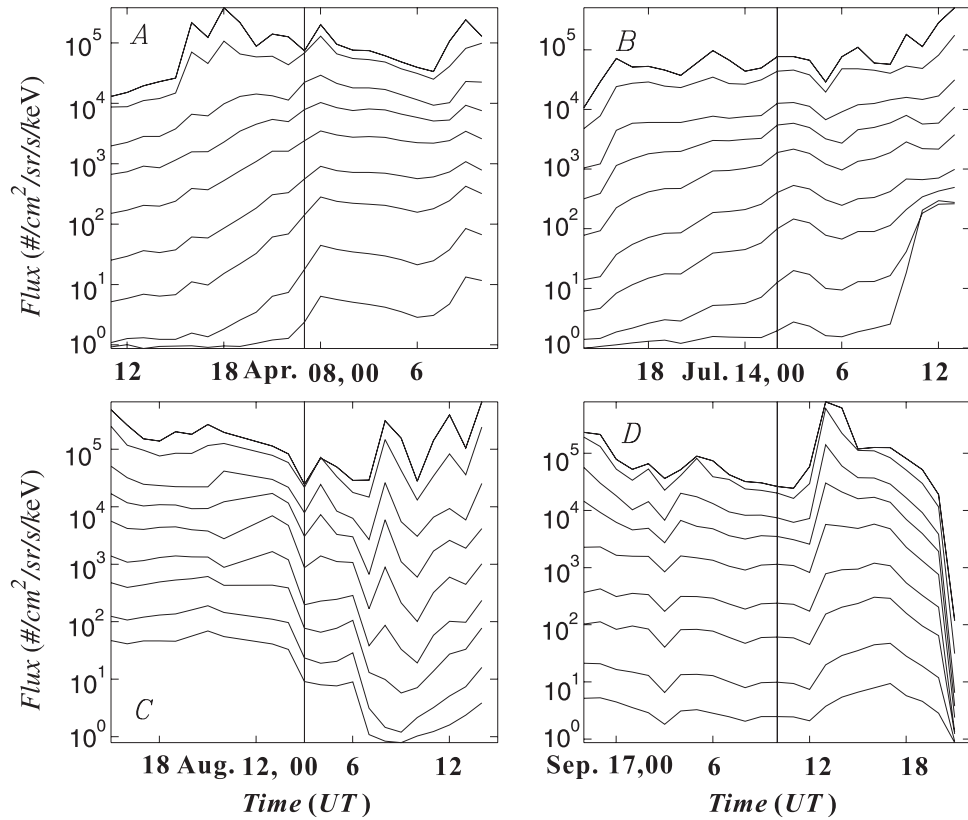


Figure 2. Plot of one-h averaged omnidirectional differential flux of energetic electrons during the different universal times (24-h interval, events A–D) from the geostationary satellite 1989-046. The time we use to fit is denoted by the solid line and locates at the center of each panel.

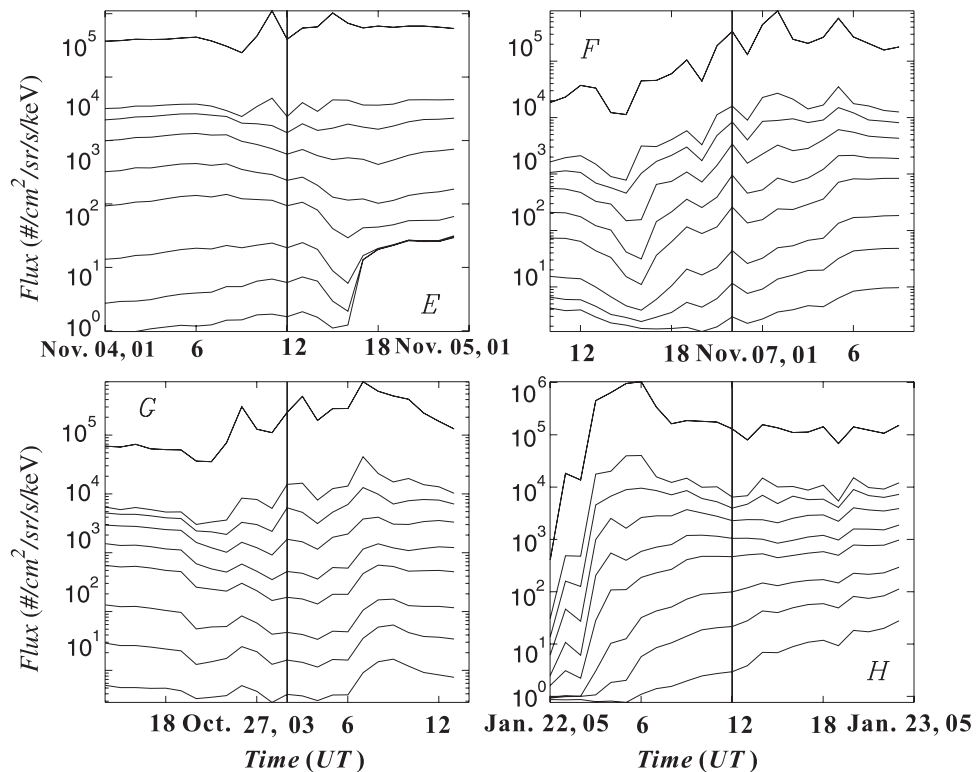


Figure 3. Same as Figure 2 except for different universal times (events E–H) and the satellite LANL-01A.

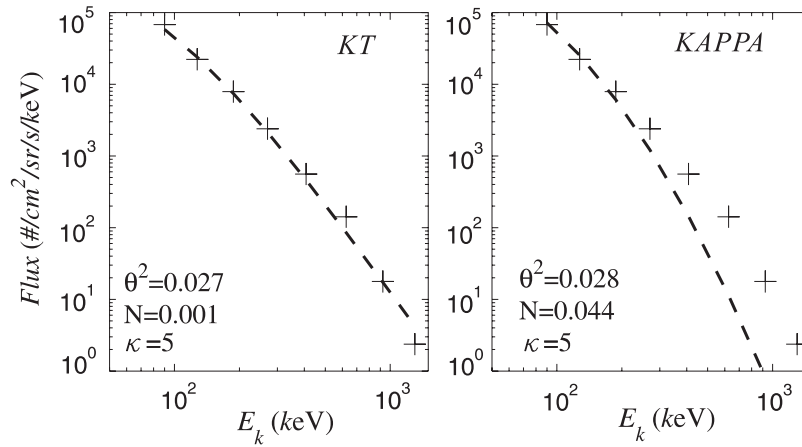


Figure 4. (right). Fitting curve (dashed line) of the omnidirectional differential flux by KT distribution with the best fitting values of parameters of θ^2 , N and κ . The discrete cross symbols show the observational data by SOPA instrument on board the 1989-046 satellite on the time of 23:00 UT 7 April 2000 (event A). (left). Fitting curve of the omnidirectional differential flux by kappa distribution with the best fitting values of parameters of θ^2 , N and κ .

nominal energy levels for electrons are the same for all satellites carrying the SOPA detectors. The SOPA instrument on board the 1989-046 and LANL-01A satellite is described in detail by *Belian et al.* [1992]. The SOPA instrument consists of three solid state detector telescopes (T1, T2 and T3) that accept particles from three different directions relative to the spacecraft spin axis and observe the electron fluxes at 10 energy ranges from 50 keV to 1.5 MeV and above. In this study, we use the omnidirectional differential flux observations from energies 50 keV to 1.5 MeV that can be obtained from the Los Alamos National Laboratory (LANL) website: <http://leadbelly.lanl.gov/>.

[16] In general, we need to consider the pitch angle distribution (PAD) of electrons for the modeling since the PADs on the dayside are predominately 90 degree peaked, while butterfly distributions more commonly seen on the nightside [*Gannon et al.*, 2007]. *Lubchich et al.* [2006] found a correlation between the omnidirectional differential flux and the directed flux by analyzing events of the LANL

satellites, which is generalized as a function of time and pitch angle itself. However, it can be seen that both the KT (5) and kappa (8) distributions basically consist of two parts (more precisely if $\theta_{\parallel} = \theta_{\perp}$ in (8)), one is associated with the energy and another with the pitch angle. Considering that the correlation (4) between the differential flux and the distribution function is linear for each given energy, we expect that perhaps an adopted isotropic PAD approximation for modeling should not influence much the energy spectra though will primarily influence the magnitude of the flux (or the number density). Hence in this study, we do not consider the anisotropy, i.e., assume $q = 0$ in (5); $l = 0$ and $\theta_{\parallel} = \theta_{\perp}$ in (8), and rewrite $p_s \rightarrow p$ and $E_s \rightarrow E$. Then equation (5) reduces to:

$$f(p) = \frac{N}{4\pi I} \left[1 + \frac{\sqrt{1+p^2} - 1}{\kappa\theta^2} \right]^{-(\kappa+1)} \quad (10)$$

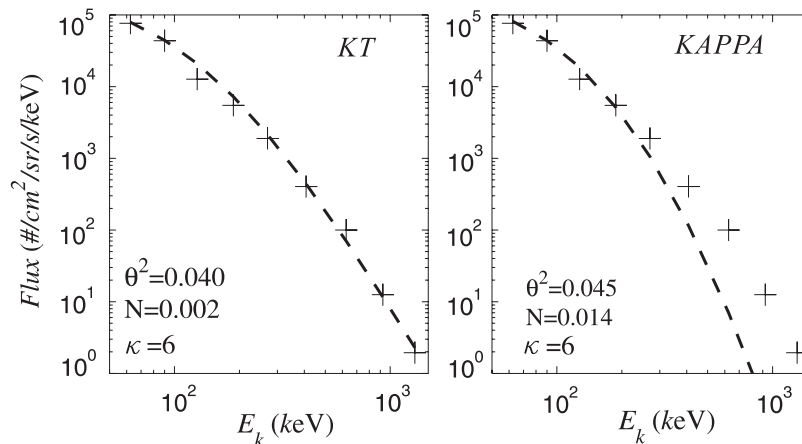


Figure 5. Same as Figure 4 except on the time of 02:00 UT 14 July 2000 (event B).

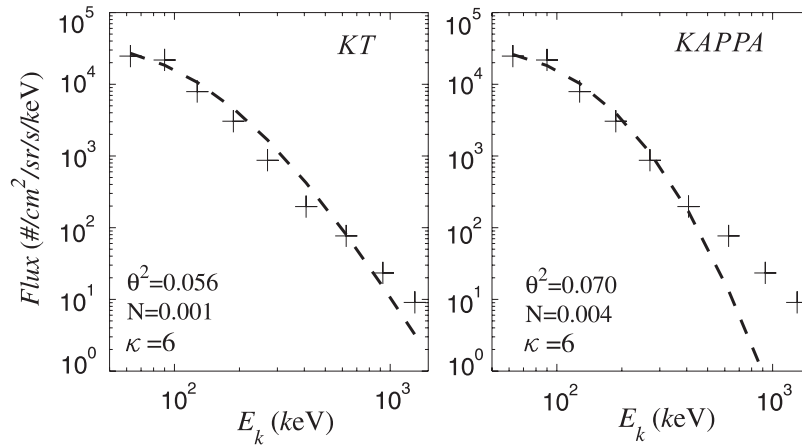


Figure 6. Same as Figure 4 except on the time of 03:00 UT 12 August 2000 (event C).

[17] Since $\sqrt{1+p^2} - 1 \approx p^2/2$ in (5) in the non-relativistic limit, here we assume $\theta_{\parallel}^2 = \theta_{\perp}^2 = 2\theta^2$ in the following calculation in order to make a consistent and direct comparison. Then equation (8) reduces to

$$f^{\kappa}(p) = \frac{\Gamma(\kappa+1)}{(2\pi)^{3/2}\theta^3\kappa^{3/2}\Gamma(\kappa-1/2)} \left[1 + \frac{p^2}{2\kappa\theta^2}\right]^{-(\kappa+1)} \quad (11)$$

[18] Figure 1 shows examples of the electron behaviors by KT distribution (10) and typical kappa distribution (11) for different indicated values of θ^2 and κ by setting $N=1$. It is shown that as θ^2 increases, the kappa distribution is found to decay faster than the KT distribution does, in particular at the higher energies. There is a turning point as θ^2 is larger (e.g., $\theta^2 \geq 20$ keV), distribution function varies slowly before the turning point and then decreases sharply after it. This suggests that the energetic electrons spectra do not follow a simple power law but depends on the electron energy range [Summers and Ma, 2000; Xiao, 2006] and the KT distribution obeys a more reasonable power law at the relativistic energies.

[19] Figures 2–3 show one-hour averaged omnidirectional differential fluxes of energetic electron during the different universal times (24-h interval in each event A–H) reported by two geostationary satellites 1989–046 and LANL-01A. Each event covers the range 75 keV to 1.5 MeV. The vertical solid line at the center of each panel corresponds to those data for fitting. We adopt such eight cases for the omnidirectional differential fluxes to be as variable as possible in order to make the results more convincing.

[20] An efficient way to do a non-linear least squared fit with a function by an arbitrary number of parameters is the typical LMFIT function in the program IDL. LMFIT function uses the Levenberg-Marquardt algorithm, which combines the steepest descent and inverse-Hessian function fitting methods [Marquardt, 1963]. By using equations (4), (10)–(11) and the LMFIT function, in Figures 4–11, we present the fitting results of the omnidirectional differential flux $j(E)$ by both the KT distribution (left panels) and the typical kappa distribution (right panels) with the best fitting values of parameters of θ^2 , N and κ (shown). The discrete cross symbols represent the observational data by the SOPA

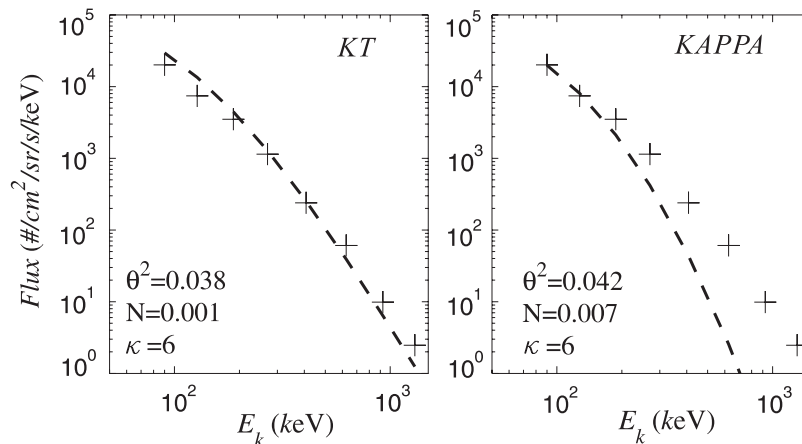


Figure 7. Same as Figure 4 except on the time of 10:00 UT 17 September 2000 (event D).

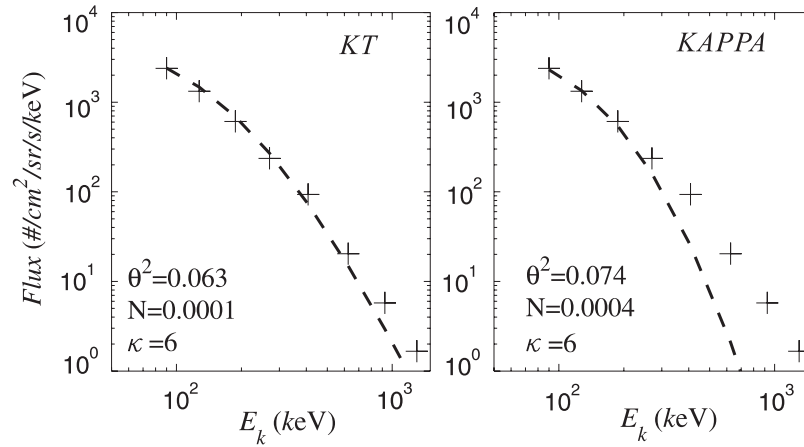


Figure 8. Same as Figure 4 except by SOPA instrument on board the LANL-01A satellite at geostationary orbit on the time of 12:00 UT 4 November 2001 (event E).

instrument on board the 1989–046 (Figures 4–7) and LANL-01A (Figures 8–11) satellites for the different indicated universal time. It is seen that the KT distribution fits well with the observational data through all the energies; whereas the kappa distribution also fits well with the observational data at lower energies but deviates from the data at higher energies, particularly above ~ 300 keV. Note that the current fitting method is quite useful since it directly gives those best fitting parameters θ^2 , N and κ which are closely associated with the calculation of instability of electromagnetic waves (e.g., the whistler mode instability). Furthermore, those fitting parameters θ^2 and N are found to be quite different for different cases due to different fluxes of electrons. However, the spectral κ is insensitive to the cases and typically takes 4, 5 or 6, consistent with previous results that the high energy tail population of the natural cosmic plasmas can be well represented by the kappa-type distribution with typical value of κ in the range of 2.0–6.0. These results above indicate that perhaps the power law spectra are ubiquitous in space plasma and the energetic electrons (particularly above hundreds of keV) may be better modeled by the KT distribution, at least in the cases of interest.

[21] For completeness, we present a quantitative analysis in Table 1 for three cases: 23:00 UT 7 April 2000, 02:00 UT 14 July 2000 and 12:00 UT 4 November 2001. We adopt a relatively error parameter:

$$\Delta = \frac{|\log_{10} j_o - \log_{10} j_f|}{\log_{10} j_o} \quad (12)$$

where j_o and j_f denotes the observed and fitted omnidirectional differential flux, respectively. Obviously, the value of the parameter Δ is found to stay in a reasonably small range for the KT distribution through the whole energy range. However, for the kappa distribution it increases gradually with the energy increasing and becomes very large particularly at MeV energies. Analysis for different cases above (which are not shown for reasons of brevity) indeed demonstrates similar results.

4. Summary and Conclusions

[22] In this paper, by adopting the condition of the isotropic PAD and a very efficient non-linear fitting method-LMFIT function in the IDL program, we have

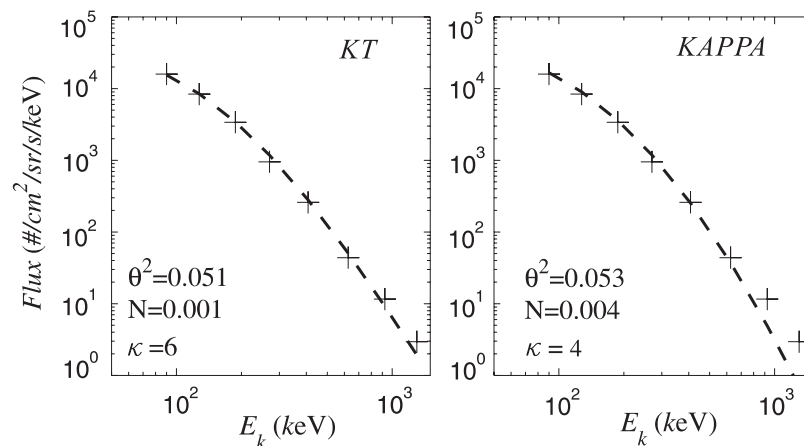


Figure 9. Same as Figure 8 except on the time of 22:00 UT 6 November 2001 (event F).

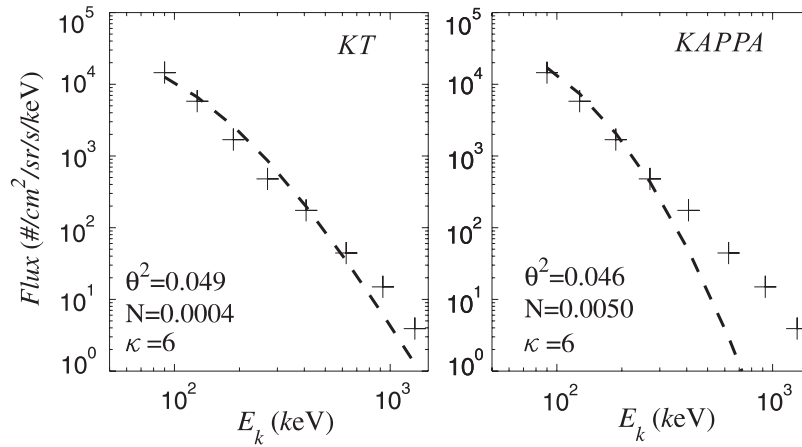


Figure 10. Same as Figure 8 except on the time of 02:00 UT 27 October 2003 (event G).

performed detailed modeling of the energetic electron spectra observed by the SOPA instrument on board the 1989–046 and LANL-01A satellites using a fully relativistic kappa-type (KT) distribution and a regular kappa distribution. We have derived a useful correlation between the differential flux and the distribution function and directly provide the best fitting results of those parameters: θ^2 , N and κ . Those parameters are strongly associated with the calculation of instability of electromagnetic waves (e.g., whistler mode wave). The following results have been obtained:

[23] (1). The energetic electron spectra from 75 keV through 1.5 MeV through all the cases of interest are well characterized by a power law which connects the low and high ends of spectrum. The fitting spectral index κ shows less variation than θ^2 and N for different cases with typical values lying in the range of 2.0–6.0. This suggests that perhaps the power law spectra are ubiquitous in space plasmas.

[24] (2). The KT distribution fits well with the observational data through all the energies from 75 keV through 1.5 MeV, indicating that highly energetic electrons (partic-

ularly above hundreds of keV) may be better modeled by the KT distribution, at least in all the cases of interest.

[25] (3). The kappa distribution also fits well with the observational data at lower energies but show deviation from the data at higher energies, particularly above ~ 300 keV. This is primarily because the kappa distribution falls off $\propto [1/v^2]^{(\kappa+1)}$ instead of $\propto [1/p]^{\kappa+1}$ at the relativistic energy, inconsistent with the power law principle.

[26] It should be aware that the current results are basically applied to the cases in which the PAD can be approximately as isotropic. However, since previous research [e.g., *Summers and Ma, 2000; Xiao, 2006*] has demonstrated that the energetic particle spectra are characterized by a complex power law which depends on the particle energy range, it is tempting to suggest that the KT distribution which follows a more reasonable power law at the relativistic energies, could be a active tool for modeling the highly energetic particles in those space plasma environments where mirror geometries occur, and even allow for future extrapolation of the processes adopted here, but this still remains to be demonstrated.

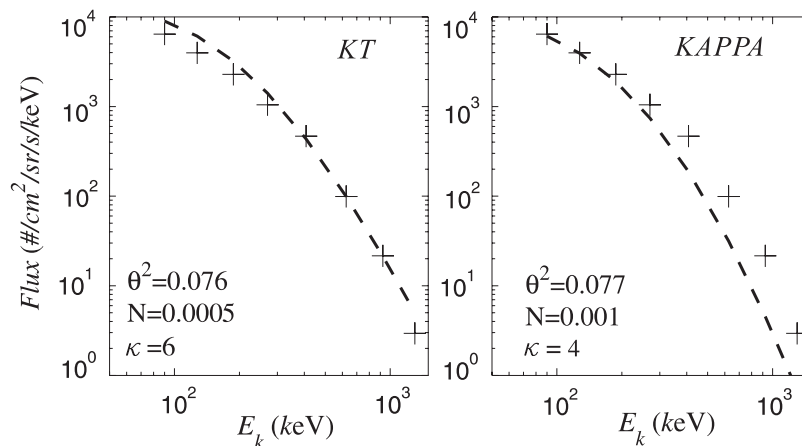


Figure 11. Same as Figure 8 except on the time of 12:00 UT 22 January 2005 (event H).

Table 1. Variations of the Relative Error Parameter Δ

Energy Range	23:00 UT 7 Apr 2000		2:00 UT 14 Jul 2000		12:00 UT 4 Nov 2001	
	Δ_{KT}	Δ_{kappa}	Δ_{KT}	Δ_{kappa}	Δ_{KT}	Δ_{kappa}
75–105keV	0.014	0.005	0.002	0.001	0.001	0.005
105–150keV	0.007	0.013	0.053	0.041	0.015	0.002
150–225keV	0.006	0.029	0.032	0.076	0.019	0.018
225–315keV	0.014	0.087	0.017	0.077	0.024	0.070
315–500keV	0.030	0.214	0.014	0.209	0.054	0.289
500–750keV	0.102	0.510	0.076	0.577	0.104	0.756
0.75–1.1MeV	0.010	1.068	0.029	1.412	0.386	2.167
1.1–1.5MeV	0.672	4.105	0.245	6.903	1.847	10.45

[27] **Acknowledgments.** This work is supported by the National Natural Science Foundation of China grants 40774078, 40774077; the Chinese Academy of Sciences Grant No. KZCX3-SW-144 and the National Key Basic Research Special Foundation of China Grant No. 2006CB806304.

[28] Zuyin Pu thanks Xinlin Li and another reviewer for their assistance in evaluating this paper.

References

- Baker, D. N. (2002), How to cope with space weather, *Science*, 297, 1486.
- Barker, A. B., X. Li, and R. S. Selesnick (2005), Modeling the radiation belt electrons with radial diffusion driven by the solar wind, *Space Weather*, 3, S10003, doi:10.1029/2004SW000118.
- Belian, R. D., G. R. Gislser, T. Cayton, and R. Christensen (1992), High-z energetic particles at geosynchronous orbit during the great solar proton event series of October 1989, *J. Geophys. Res.*, 97(A11), 16,897–16,906.
- Burin des Roziers, E., and X. Li (2006), Specification of >2 MeV geosynchronous electrons based on solar wind measurements, *Space Weather*, 4, S06007, doi:10.1029/2005SW000177.
- Callis, L. B., M. Natarajan, D. S. Evans, and J. D. Lambeth (1998), Solar atmospheric coupling by electrons (SOLACE): 1. Effects of the May 12, 1997 solar event on the middle atmosphere, *J. Geophys. Res.*, 103(D21), 28,405–28,419.
- Christon, S. P., D. G. Mitchell, D. J. Williams, L. A. Frank, and H. C. Y. Eastman (1988), Energy spectra of plasmasheet ions and electrons from 50 eV/e to 1 mev during plasma temperature transitions, *J. Geophys. Res.*, 93(A4), 2562–2572.
- Dasso, S., F. T. Gratton, and C. J. Farrugia (2003), A parametric study of the influence of ion and electron properties on the excitation of electromagnetic ion cyclotron waves in coronal mass ejections, *J. Geophys. Res.*, 108(A4), 1149, doi:10.1029/2002JA009558.
- Freeman, J. W., T. P. O'Brien, A. A. Chan, and R. A. Wolf (1998), Energetic electrons at geostationary orbit during the November 3–4 storm: Spatial/temporal morphology, characterization by a power law and, representation by an artificial neural network, *J. Geophys. Res.*, 103(A11), 26,251–26,260.
- Gannon, J. L., X. Li, and D. Heynderickx (2007), Pitch angle distribution analysis of radiation belt electrons based on combined release and radiation effects satellite medium electrons a data, *J. Geophys. Res.*, 112, A05212, doi:10.1029/2005JA011565.
- Gary, S. P., and J. Wang (1996), Whistler instability: Electron anisotropy upper bound, *J. Geophys. Res.*, 101(A5), 10,749–10,754.
- Gary, S. P., D. Winske, and M. Hesse (2000), Electron temperature anisotropy instabilities: Computer simulations, *J. Geophys. Res.*, 105(A5), 10,751–10,759.
- Gary, S. P., B. Lavraud, M. F. Thomsen, B. Lefebvre, and S. J. Schwartz (2005), Electron anisotropy constraint in the magnetosheath: Cluster observations, *Geophys. Res. Lett.*, 32, L13109, doi:10.1029/2005GL023234.
- Gendrin, R. (2001), The role of wave particle interactions in radiation belts modeling, in *Sun-Earth Connection and Space Weather*, vol. 75, p. 151, It. Phys. Soc., Bologna.
- Gladd, N. T. (1983), The whistler instability at relativistic energies, *Phys. Fluids*, 26, 974.
- Horne, R. B. (2002), The contribution of wave-particle interactions to electron loss and acceleration in the Earth's radiation belts during geomagnetic storms, in *Review of Radio Science 1999–2002*, vol. 33, p. 801, John Wiley, Hoboken, N. J.
- Horne, R. B., S. A. Glauert, and R. M. Thorne (2003a), Resonant diffusion of radiation belt electrons by whistler mode chorus, *Geophys. Res. Lett.*, 30(9), 1493, doi:10.1029/2003GL016963.
- Horne, R. B., R. M. Thorne, N. P. Meredith, and R. R. Anderson (2003b), Diffuse auroral electron scattering by electron cyclotron harmonic and whistler mode waves during an isolated substorm, *J. Geophys. Res.*, 108(A7), 1290, doi:10.1029/2002JA009736.
- Horne, R. B., R. M. Thorne, S. A. Glauert, J. M. Albert, N. P. Meredith, and R. R. Anderson (2005a), Timescale for radiation belt electron acceleration by whistler mode chorus waves, *J. Geophys. Res.*, 110, A03225, doi:10.1029/2004JA010811.
- Horne, R. B., et al. (2005b), Wave acceleration of electrons in the van Allen radiation belts, *Nature*, 437, 227.
- Li, X. (2004), Variations of 0.7–6.0 MeV electrons at geosynchronous orbit as a function of solar wind, *Space Weather*, 2, S03006, doi:10.1029/2003SW000017.
- Li, X., and M. A. Temerin (2001), The electron radiation belt, *Space Sci. Rev.*, 95, 569.
- Li, X., et al. (1997), Multisatellite observations of the outer zone electron variation during the November 3–4, 1993, magnetic storm, *J. Geophys. Res.*, 102(A7), 14,123–14,140.
- Li, X., et al. (1999), Rapid enhancements of relativistic electrons deep in the magnetosphere during the may 15, 1997 magnetic storm, *J. Geophys. Res.*, 104(A3), 4467–4476.
- Li, X., M. Temerin, D. N. Baker, G. D. Reeves, and D. Larson (2001), Quantitative prediction of radiation belt electrons at geostationary orbit based on solar wind measurements, *Geophys. Res. Lett.*, 28(9), 1887–1890.
- Li, L., J. Cao, and G. Zhou (2005a), Combined acceleration of electrons by whistler-mode and compressional ULF turbulences near the geosynchronous orbit, *J. Geophys. Res.*, 110, A03203, doi:10.1029/2004JA010628.
- Li, X., D. N. Baker, M. Temerin, G. D. Reeves, R. Friedel, and C. Shen (2005b), Energetic electrons, 50 keV–6 MeV, at geosynchronous orbit: Their responses to solar wind variations, *Space Weather*, 3, S04001, doi:10.1029/2004SW000105.
- Lubchich, A. A., A. G. Yahnin, E. E. Titova, A. G. Demekhov, V. Y. Trakhtengerts, J. Manninen, and T. Turunen (2006), Longitudinal drift of substorm electrons as the reason of impulsive precipitation events and VLF emissions, *Ann. Geophys.*, 24, 2667.
- Ma, C., and D. Summers (1998), Formation of power-law energy spectra in space plasmas by stochastic acceleration due to whistler-mode waves, *Geophys. Res. Lett.*, 25(21), 4099–4102.
- Maksimovic, M., V. Pierrard, and J. F. Lemaire (1997a), A kinetic model of the solar wind with kappa distribution functions in the corona, *Astron. Astrophys.*, 324, 725.
- Maksimovic, M., V. Pierrard, and P. Riley (1997b), Ulysses electron distributions fitted with kappa functions, *Geophys. Res. Lett.*, 24(9), 1151–1154.
- Marquardt, D. W. (1963), An algorithm for least-squares estimation of nonlinear parameters, *J. Soc. Indust. Appl. Math.*, 11, 431.
- Meredith, N. P., R. B. Horne, R. H. A. Iles, R. M. Thorne, R. R. Anderson, and D. Heynderickx (2002), Outer zone relativistic electron acceleration associated with substorm enhanced whistler mode chorus, *J. Geophys. Res.*, 107(A7), 1144, doi:10.1029/2001JA900146.
- Meredith, N. P., M. Cain, R. B. Horne, R. M. Thorne, D. Summers, and R. R. Anderson (2003a), Evidence for chorus driven electron acceleration to relativistic energies from a survey of geomagnetically disturbed periods, *J. Geophys. Res.*, 108(A6), 1248, doi:10.1029/2002JA009764.
- Meredith, N. P., R. M. Thorne, R. B. Horne, D. Summers, B. J. Fraser, and R. R. Anderson (2003b), Statistical analysis of relativistic electron energies for cyclotron resonance with EMIC waves observed on CRRES, *J. Geophys. Res.*, 108(A6), 1250, doi:10.1029/2002JA009700.
- Reames, D. V., L. M. Barbier, T. T. von Roseninge, G. M. Mason, J. E. Mazur, and J. R. Dwyer (1997), Energy spectra of ions accelerated in impulsive and gradual solar events, *Astrophys. J.*, 483, 515.
- Reeves, G. D., et al. (1998), The relativistic electron response at geosynchronous orbit during the January 1997 magnetic storm, *J. Geophys. Res.*, 103(A8), 17,559–17,570.
- Reeves, G. D., K. L. McAdams, R. H. W. Friedel, and T. P. O'Brien (2003), Acceleration and loss of relativistic electrons during geomagnetic storms, *Geophys. Res. Lett.*, 30(10), 1529, doi:10.1029/2002GL016513.
- Roth, I., M. Temerin, and M. K. Hudson (1999), Resonant enhancement of relativistic electron fluxes during geomagnetically active periods, *Ann. Geophys.*, 17, 631.
- Saito, S., F. R. E. Forne, S. C. Buchert, S. Nozawa, and R. Fujii (2000), Effects of kappa distribution electrons on incoherent scatter spectra, *Ann. Geophys.*, 18, 1054.
- Sarris, T., X. Li, and M. Temerin (2006), Simulating radial diffusion of energetic (MeV) electrons through a model of fluctuating electric and magnetic fields, *Ann. Geophys.*, 24, 1.
- Schlickeiser, R., H. Fichtner, and M. Kneller (1997), Revised landau damping rates of magnetohydrodynamic waves in hot magnetized equilibrium plasmas and its consequences for cosmic ray transport in the interplanetary medium, *J. Geophys. Res.*, 102(A3), 4725–4739.
- Schulz, M., and L. J. Lanzerotti (1974), Particle diffusion in the radiation belts, in *Physics and Chemistry in Space*, vol. 7, Springer-Verlag, New York.

- Summers, D., and C. Ma (2000), A model for generating relativistic electrons in the Earth's inner magnetosphere based on gyroresonant wave-particle interactions, *J. Geophys. Res.*, *105*(A2), 2625–2639.
- Summers, D., and R. M. Thorne (2003), Relativistic electron pitch-angle scattering by electromagnetic ion cyclotron waves during geomagnetic storms, *J. Geophys. Res.*, *108*(A4), 1143, doi:10.1029/2002JA009489.
- Summers, D., R. M. Thorne, and F. Xiao (1998), Relativistic theory of wave-particle resonant diffusion with application to electron acceleration in the magnetosphere, *J. Geophys. Res.*, *103*(A9), 20,487–20,500.
- Summers, D., R. M. Thorne, and F. Xiao (2001), Gyroresonant acceleration of electrons in the magnetosphere by superluminous electromagnetic waves, *J. Geophys. Res.*, *106*(A6), 10,853–10,868.
- Summers, D., C. Ma, N. P. Meredith, R. B. Horne, R. M. Thorne, and R. R. Anderson (2004), Modeling outer-zone relativistic electron response to whistler mode chorus activity during substorms, *J. Atmos. Sol. Terr. Phys.*, *66*, 133.
- Summers, D., B. Ni, and N. P. Meredith (2007a), Timescales for radiation belt electron acceleration and loss due to resonant wave-particle interactions: 1. Theory, *J. Geophys. Res.*, *112*, A04206, doi:10.1029/2006JA011801.
- Summers, D., B. Ni, and N. P. Meredith (2007b), Timescales for radiation belt electron acceleration and loss due to resonant wave-particle interactions: 2. Evaluation for vlf chorus, elf hiss, and electromagnetic ion cyclotron waves, *J. Geophys. Res.*, *112*, A04207, doi:10.1029/2006JA011993.
- Thorne, R. M. (1977), Energetic radiation belt electron precipitation: A natural depletion mechanism for stratospheric ozone, *Science*, *195*, 287.
- Thorne, R. M., R. B. Horne, S. A. Glauert, N. P. Meredith, Y. Shprits, D. Summers, and R. R. Anderson (2005a), The influence of wave-particle interactions on relativistic electron dynamics during storms, in *Inner Magnetosphere Interactions: New Perspectives From Imaging*, *Geophys. Monogr. Ser.*, vol. 159, p. 101, AGU, Washington, D.C.
- Thorne, R. M., T. P. O'Brien, Y. Y. Shprits, D. Summers, and R. B. Horne (2005b), Timescale for MeV electron microburst loss during geomagnetic storms, *J. Geophys. Res.*, *110*, A09202, doi:10.1029/2004JA010882.
- Vasyliunas, V. M. (1968), A survey of low-energy electrons in the evening sector of the magnetosphere with ogo 1 and ogo 3, *J. Geophys. Res.*, *73*(9), 2839–2884.
- Viñas, A. F., R. L. Mace, and R. F. Benson (2005), Dispersion characteristics for plasma resonances of Maxwellian and kappa distribution plasmas and their comparisons to the image/rpi observations, *J. Geophys. Res.*, *110*, A06202, doi:10.1029/2004JA010967.
- Xiao, F. (2006), Modelling energetic particles by a relativistic kappa loss cone distribution function in plasmas, *Plasma Phys. Controlled Fusion*, *48*, 203.
- Xiao, F., R. M. Thorne, and D. Summers (1998), Instability of electromagnetic r-mode waves in a relativistic plasma, *Phys. Plasmas*, *5*, 2489.
- Xiao, F., Q. H. Zhou, H. Y. He, H. N. Zheng, and S. Wang (2006a), Relativistic diffusion coefficients for superluminous (auroral kilometric radiation) wave modes in space plasmas, *J. Geophys. Res.*, *111*, A11201, doi:10.1029/2006JA011865.
- Xiao, F., Q. H. Zhou, H. N. Zheng, and S. Wang (2006b), Whistler instability threshold condition of energetic electrons by kappa distribution in space plasmas, *J. Geophys. Res.*, *111*, A08208, doi:10.1029/2006JA011612.
- Xiao, F., Q. H. Zhou, H. Y. He, and L. J. Tang (2006c), Instability of whistler-mode waves by a relativistic kappa-loss-cone distribution in space plasmas, *Plasma Phys. Controlled Fusion*, *48*, 1437.
- Xiao, F., R. M. Thorne, and D. Summers (2007a), Higher-order gyroresonant acceleration of electrons by superluminous (AKR) wave-modes, *Planet. Space Sci.*, *55*, 1257.
- Xiao, F., Q. H. Zhou, H. Y. He, H. N. Zheng, and S. Wang (2007b), Electromagnetic ion cyclotron waves instability threshold condition of suprathermal protons by kappa distribution, *J. Geophys. Res.*, *112*, A07219, doi:10.1029/2006JA012050.
- Xue, S., R. M. Thorne, and D. Summers (1993), Electromagnetic ion-cyclotron instability in space plasmas, *J. Geophys. Res.*, *98*(A10), 17,475–17,484.
- Zong, Q.-G., et al. (2007), Ultralow frequency modulation of energetic particles in the dayside magnetosphere, *Geophys. Res. Lett.*, *34*, L12105, doi:10.1029/2007GL029915.

C. Shen, S. Wang, Y. Wang, and H. Zheng, Department of Earth and Space Sciences, University of Science and Technology of China, Hefei 230026, China. (clshen@mail.ustc.edu.cn; swan@ustc.edu.cn; ymwang@ustc.edu.cn; hue@ustc.edu.cn)

F. Xiao, School of Physics and Electronic Sciences, Changsha University of Science and Technology, Changsha 410076, China. (flxiao@126.com)